METHODS

Sites identified within the K-feldspar overgrowths to be sampled for TEM work were selected by backscattered electron imaging of carbon coated polished thin sections (Fig. 2B). Following sputter coating with ~ 40 nm of gold, electron-transparent (i.e., 100 nm thick) foils were cut from the overgrowths with a FEI 200TEM FIB instrument using 30 kV Ga^+ ions. The ion milling process is described in detail by Heaney et al. (2001) and Lee et al. (2003). Following extraction from the thin section using an ex-situ micromanipulator, the foils were placed on a holey carbon film and imaged using a FEI T20 TEM operated at 200 kV. With respect to the method presented by Mark et al. (2005) the preparation of TEM foils using the FIB technique is the major advancement. With a high degree of precision and accuracy we can sample any section of a K-feldspar overgrowth.

Doubly polished fluid inclusion wafers, 100 µm thick, were prepared from core samples and characterized (homogenization [T_h] and final ice melting [T_m] temperatures determined) using a calibrated (associated error, ± 1 °C) Linkam TH-600 fluid inclusion stage with a heating rate of 10 °C min^{-1}. All fluid inclusions showed consistent sizes, shapes, vapor bubble sizes, and vapor-liquid ratios. Inclusions that showed stretching were excluded from the study. T_m measurements were determined using a heating rate of 1 °C min^{-1}. Salinities were estimated using the methods of Bodnar (1993).

Prior to irradiation, a 100 µm thick doubly polished fluid inclusion wafer was cleaned ultrasonically in methanol and deionised water. The sample was cadmium shielded (3 mm) and irradiated for 50 hours in the McMaster reactor in Canada. Neutron flux was monitored with biotite standard GA1550 (~ 98.8 ± 0.5 Ma; McDougall & Roksandic, 1974; Renne et al., 1998; Spell & McDougall, 2003); resulting in a J value of 0.01175 ± 0.000006 was used. A New Wave Research UP-213 nm pulsed Nd-YAG laser with a 12 µm spot size (rastered over the surface to obtain sufficient gas for precise isotope measurements) was used for Ar extraction. Extracted gases were cleaned using three SAES AP10 getters, two operated at 450 °C and one at room temperature. A MAP 215-50 noble gas mass spectrometer analysed Ar isotope compositions. The data were corrected for blanks, mass spectrometer discrimination, ^{37}Ar decay and reactor induced interferences. Quoted Ar-Ar errors are 2σ and include a 0.5 % error assigned to the J value. Reactor induced correction factors used were: $(^{39}Ar/^{37}Ar)_{Ca}$ = 0.00065, $(^{36}Ar/^{37}Ar)_{Ca}$ = 0.000264, $(^{40}Ar/^{39}Ar)_{K}$ = 0.0085. Mark et al. (2006) provides details concerning the integration of fluid inclusion and age data. The decay constants as outline by Steiger and Jager (1977) were used. We use the timescale of Gradstein et al. (2004).

Thermal history data was input into a finite element diffusion model DIFFARG (Wheeler, 1996) which works with MATLAB® software. The programme allows modelling of Ar diffusion with respect to a precise thermal history. Effective diffusion domain size was inputted for a series of geometrical shapes of different sizes (determined using TEM imaging). Their response to the thermal history over time was tested. DIFFARG is a forward modelling programme and hence, 0 Ma corresponds to the age of K-feldspar authigenesis.

References:

Bodnar, B.J., (1993) Revised equation and table for determining the freezing point depression of H2O-NaCl solutions. Geochimica et Cosmochimica Acta, 57, 683-684.

Gradstein, F.M., Ogg, J.G. & Smith, A.G., (2004) A geologic time scale. Cambridge, p610.

Heaney, P.J., Vincenzi, E.P., Giannuzzi, L.A. & Livi, K.J.T., (2001) Focussed ion beam milling: a method of site specific sample extraction for microanalysis of Earth and planetary materials. American Mineralogist, 86, 1094-1099.

Lee, M.R., Bland, P.A. & Graham, G., (2003) Preparation of TEM samples by focused ion beam (FIB) techniques: applications to the study of clays and phyllosilicates in meteorites. Mineralogical Magazine, 67, 581-592.

McDougall, I. & Roksandic, Z., (1974) Total fusion $^{40}Ar/^{39}Ar$ ages using HIFAR reactor. Geological Society of Australia Journal, 21, 81-89.

Mark, D.F., Parnell, J., Kelley, S.P., Lee, M., Sherlock, S.C., and Carr, A., 2005, Dating of Multistage Fluid Flow in Sandstone: Science, v. 309, p. 2048–2051.

Mark, D.F., Parnell, J., Kelley, S.P. & Sherlock, S.C., (2006) Temperature-composition-time (TXt) data from authigenic K-feldspar: an integrated methodology for dating fluid flow events. Journal of Geochemical Exploration, 89, 259-262.

Renne, P.R., Swisher, C.C., Deino, A.L., Karner, D.B., Owens, T.L. & DePaolo, D.J., (1998) Intercalibration of standards, absolute ages and uncertainties in Ar/Ar dating. Chemical Geology, 145, 117-152.

Spell, T.L. & McDougall, I., (2003) Characterization and calibration of $^{40}Ar/^{39}Ar$ dating standards. Chemical Geology, 198, 189-211.

Steiger, R.H. & Jager, E., (1977) Subcommision on Geochronology: convention on the use of decay constants in geo- and cosmochronology. Earth and Planetary Science Letters, 36, 359-362.

Wheeler, J., (1996) DIFFARG: A program for stimulating argon diffusion profiles in minerals. Computers & Geosciences, 22, (8), 919-929.

Table DR1: Primary aqueous 2-phase (liquid and vapour) fluid inclusion micro-thermometric data from authigenic K-feldspar overgrowths.

Inclusion ref	Size (µm)	Mineral host	Inclusion type	Phases	T_h (°C)	T_m (°C)	Salinity (wt. % NaCl eq.)
1	8	K-feldspar	Primary	2 (liquid & vapour)	167.8	-6.5	9.9
2	7	K-feldspar	Primary	2 (liquid & vapour)	155.4	-7.1	10.6
3	6	K-feldspar	Primary	2 (liquid & vapour)	159.3	-6.8	10.2
4	9	K-feldspar	Primary	2 (liquid & vapour)	163.7	-6.1	9.3
5	8	K-feldspar	Primary	2 (liquid & vapour)	165.4	-6.2	9.5
6	9	K-feldspar	Primary	2 (liquid & vapour)	155.2	-6.5	9.9
7	10	K-feldspar	Primary	2 (liquid & vapour)	158.2	-6.7	10.1
8	4	K-feldspar	Primary	2 (liquid & vapour)	154.1	-6.4	9.7
9	5	K-feldspar	Primary	2 (liquid & vapour)	167.3	-7.3	10.9
10	8	K-feldspar	Primary	2 (liquid & vapour)	164.7	-7.1	10.6
11	7	K-feldspar	Primary	2 (liquid & vapour)	161.1	-6.7	10.1
12	6	K-feldspar	Primary	2 (liquid & vapour)	163.7	-6.4	9.7
13	4	K-feldspar	Primary	2 (liquid & vapour)	154.8	-6.6	10.0
14	4	K-feldspar	Primary	2 (liquid & vapour)	160.0	-6.8	10.2
15	5	K-feldspar	Primary	2 (liquid & vapour)	162.5	-6.8	10.2
16	9	K-feldspar	Primary	2 (liquid & vapour)	166.7	-6.6	10.0
17	7	K-feldspar	Primary	2 (liquid & vapour)	158.2	-6.8	10.2
18	6	K-feldspar	Primary	2 (liquid & vapour)	155.9	-6.7	10.1
19	4	K-feldspar	Primary	2 (liquid & vapour)	154.7	-6.1	9.3
20	8	K-feldspar	Primary	2 (liquid & vapour)	163.7	-7.0	10.5
21	6	K-feldspar	Primary	2 (liquid & vapour)	159.2	-7.3	10.9
22	7	K-feldspar	Primary	2 (liquid & vapour)	165.5	-6.5	9.9
23	5	K-feldspar	Primary	2 (liquid & vapour)	158.9	-6.8	10.2
24	6	K-feldspar	Primary	2 (liquid & vapour)	163.2	-6.9	10.4
25	9	K-feldspar	Primary	2 (liquid & vapour)	167.6	-7.2	10.7
26	10	K-feldspar	Primary	2 (liquid & vapour)	160.2	-7.1	10.6
27	8	K-feldspar	Primary	2 (liquid & vapour)	155.3	-6.3	9.6
28	7	K-feldspar	Primary	2 (liquid & vapour)	158.7	-6.7	10.1
29	4	K-feldspar	Primary	2 (liquid & vapour)	161.1	-6.9	10.4
30	4	K-feldspar	Primary	2 (liquid & vapour)	166.3	-7.2	10.7
31	5	K-feldspar	Primary	2 (liquid & vapour)	159.4	-6.1	9.3
32	7	K-feldspar	Primary	2 (liquid & vapour)	158.2	-6.4	9.7
33	8	K-feldspar	Primary	2 (liquid & vapour)	158.7	-6.3	9.6
34	9	K-feldspar	Primary	2 (liquid & vapour)	154.2	-7.0	10.5
35	7	K-feldspar	Primary	2 (liquid & vapour)	160.3	-6.7	10.1
36	8	K-feldspar	Primary	2 (liquid & vapour)	165.8	-7.2	10.7
37	6	K-feldspar	Primary	2 (liquid & vapour)	166.2	-6.7	10.1
38	5	K-feldspar	Primary	2 (liquid & vapour)	163.5	-6.6	10.0
39	8	K-feldspar	Primary	2 (liquid & vapour)	163.9	-6.5	9.9
40	5	K-feldspar	Primary	2 (liquid & vapour)	164.5	-6.3	9.6
41	8	K-feldspar	Primary	2 (liquid & vapour)	167.7	-6.1	9.3

Table DR2: $^{40}Ar/^{39}Ar$ data from authigenic K-feldspar overgrowths (volts) from well 204/28-1 sampled at a depth of 1919.1 m. All errors are quoted as 2σ.

run No	40bk	±	39bk	±	38bk	±	37bk	±	36bk	±
W05A13459	0.04666	0.00048	0.00022	0.00002	0.00018	0.00001	0.00595	0.00005	0.00058	0.00001
W05A13477	0.04949	0.00018	0.00052	0.00002	0.00025	0.00001	0.00697	0.00006	0.00086	0.00001
W05A13479	0.05005	0.00036	0.00051	0.00002	0.00025	0.00001	0.00692	0.00005	0.00087	0.00002
W05A13481	0.04689	0.00024	0.00054	0.00002	0.00022	0.00002	0.00679	0.00003	0.00083	0.00003
W05A13507	0.03359	0.00031	0.00078	0.00002	0.00025	0.00000	0.00572	0.00006	0.00074	0.00001
W05A13526	0.03367	0.00034	0.00095	0.00002	0.00023	0.00002	0.00614	0.00004	0.00077	0.00001
W05A13536	0.03018	0.00021	0.00091	0.00002	0.00023	0.00001	0.00556	0.00005	0.00067	0.00002
W05A13538	0.03170	0.00021	0.00082	0.00002	0.00025	0.00002	0.00593	0.00005	0.00072	0.00003
W05A13542	0.03136	0.00015	0.00097	0.00002	0.00019	0.00001	0.00539	0.00003	0.00086	0.00002
W05A13544	0.03185	0.00031	0.00131	0.00002	0.00022	0.00001	0.00539	0.00010	0.00097	0.00002
W05A13546	0.03219	0.00020	0.00122	0.00002	0.00024	0.00000	0.00552	0.00003	0.00094	0.00002
W05A13548	0.03254	0.00015	0.00099	0.00002	0.00025	0.00000	0.00573	0.00007	0.00085	0.00001
W05A13554	0.03244	0.00026	0.00121	0.00002	0.00017	0.00002	0.00642	0.00004	0.00096	0.00002
W05A13556	0.03265	0.00022	0.00148	0.00002	0.00021	0.00002	0.00617	0.00003	0.00104	0.00002
W05A13558	0.03197	0.00036	0.00155	0.00002	0.00021	0.00001	0.00588	0.00006	0.00099	0.00001
W05A13562	0.03110	0.00019	0.00139	0.00002	0.00028	0.00001	0.00631	0.00007	0.00093	0.00001
W05A13564	0.03036	0.00018	0.00143	0.00002	0.00026	0.00001	0.00616	0.00006	0.00090	0.00002
W05A13571	0.02626	0.00032	0.00027	0.00002	0.00020	0.00000	0.00579	0.00003	0.00060	0.00001

Table DR2.1: Blank measurement for each individual analysis.

run No	40Ar	+-	39Ar	+-	38Ar	+-	37Ar	+-	36Ar	+-	40Ar*/39Ar	+-	Age (Ma)	+-
W05A13459	0.06724	0.00056	0.01323	0.00004	0.00014	0.00002	-0.00234	0.00044	0.00010	0.00003	5.08	0.67	104.38	13.41
W05A13477	0.05605	0.00034	0.01124	0.00006	0.00018	0.00001	0.00148	0.00034	0.00010	0.00003	4.99	0.79	102.52	15.79
W05A13479	0.06214	0.00046	0.01047	0.00012	0.00010	0.00001	0.00188	0.00030	0.00010	0.00003	5.93	0.85	121.31	16.83
W05A13481	0.07679	0.00031	0.01368	0.00009	0.00025	0.00002	0.00391	0.00020	0.00010	0.00003	5.61	0.65	114.92	12.89
W05A13507	0.07169	0.00032	0.01245	0.00010	0.00011	0.00002	-0.00072	0.00037	0.00010	0.00004	5.76	0.95	117.77	18.84
W05A13526	0.07355	0.00038	0.01331	0.00007	0.00004	0.00002	-0.00108	0.00024	0.00010	0.00004	5.53	0.89	113.24	17.67
W05A13536	0.10701	0.00023	0.01939	0.00008	0.00026	0.00002	0.00015	0.00031	0.00010	0.00003	5.52	0.46	113.07	9.11
W05A13538	0.08031	0.00027	0.01520	0.00011	0.00013	0.00002	-0.00092	0.00026	0.00010	0.00003	5.28	0.58	108.38	11.65
W05A13542	0.06421	0.00040	0.01189	0.00008	0.00006	0.00001	-0.00219	0.00032	0.00010	0.00003	5.40	0.75	110.76	14.87
W05A13544	0.07622	0.00035	0.01415	0.00006	0.00010	0.00003	0.00214	0.00056	0.00010	0.00003	5.39	0.63	110.46	12.49
W05A13546	0.07502	0.00023	0.01505	0.00004	0.00022	0.00002	0.00124	0.00050	0.00010	0.00003	4.99	0.59	102.45	11.79
W05A13548	0.07873	0.00017	0.00995	0.00007	0.00008	0.00002	0.00158	0.00037	0.00010	0.00003	4.94	0.89	101.55	17.82
W05A13554	0.08776	0.00027	0.01469	0.00004	0.00012	0.00002	-0.00166	0.00035	0.00010	0.00003	5.97	0.60	122.08	11.95
W05A13556	0.07165	0.00025	0.01258	0.00009	0.00016	0.00002	0.00029	0.00017	0.00010	0.00003	5.69	0.71	116.55	14.01
W05A13558	0.07883	0.00048	0.01321	0.00008	0.00022	0.00001	0.00317	0.00032	0.00010	0.00003	5.97	0.67	121.93	13.31
W05A13562	0.07723	0.00039	0.01223	0.00007	0.00025	0.00001	0.00259	0.00039	0.00010	0.00003	6.32	0.73	128.84	14.32
W05A13564	0.06894	0.00033	0.01224	0.00007	0.00005	0.00001	0.00054	0.00045	0.00010	0.00003	5.63	0.73	115.30	14.40
W05A13571	0.09932	0.00046	0.01784	0.00007	0.00027	0.00001	-0.00084	0.00021	0.00010	0.00003	5.57	0.50	114.05	9.90

Table DR2.2: Raw Ar-Ar data for authigenic K-feldspar overgrowths (n=18). Data are corrected for blanks and mass discrimination.

Table DR3: Integrated TXt data from 18 K-feldspar overgrowths that were targeted for fluid inclusion microthermometry and ^{40}Ar-^{39}Ar analysis.

REF	T_h (°C)	Salinity (wt. %	Age (Ma)	+/-
TXt 1	167.8	9.9	104.4	13.4
TXt 2	155.4	10.6	102.5	15.8
TXt 3	159.3	10.2	121.3	16.8
TXt 4	163.7	9.3	114.9	12.9
TXt 5	165.4	9.5	117.8	18.8
TXt 6	155.2	9.9	113.2	17.7
TXt 7	158.2	10.1	113.1	9.1
TXt 8	154.1	9.7	108.4	11.7
TXt 9	167.3	10.9	110.8	14.9
TXt 10	164.7	10.6	110.5	12.5
TXt 11	161.1	10.1	102.5	11.8
TXt 12	163.7	9.7	101.6	17.8
TXt 13	154.8	10.0	122.1	11.9
TXt 14	160.0	10.2	116.6	14.0
TXt 15	162.5	10.2	121.9	13.3
TXt 16	166.7	10.0	128.8	14.3
TXt 17	158.2	10.2	115.3	14.4
TXt 18	155.9	10.1	114.0	9.9

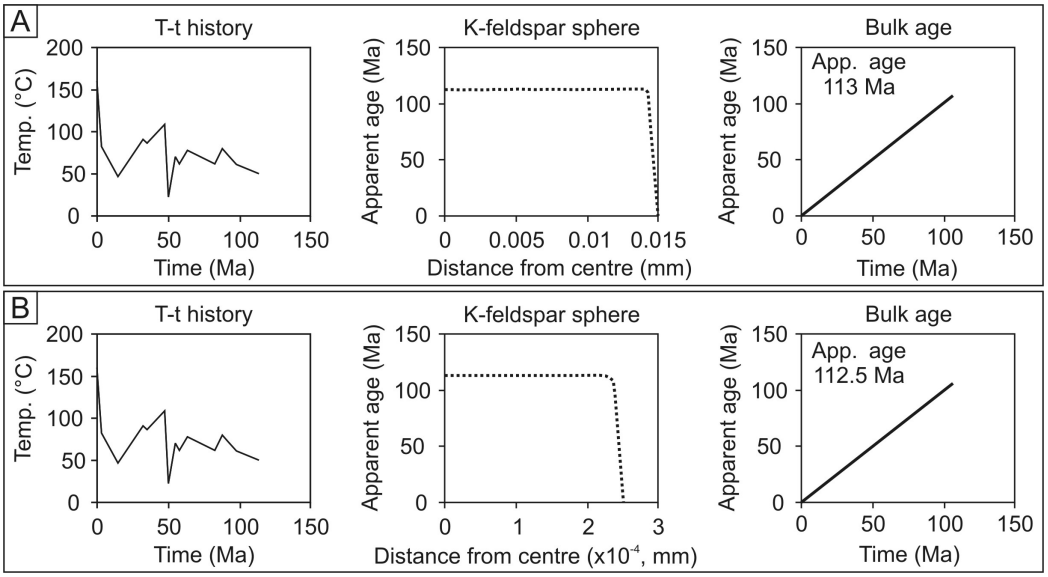

Figure DR1: DIFFARG model output showing temperature-time (T-t) history, a diffusion profile through a K-feldspar spherical crystal and the sample bulk age. (A) Using an authigenic K-feldspar overgrowth thickness (30 μm) as the effective diffusion dimension shows that no significant radiogenic ^{40}Ar has been lost. (B) Using a subgrain size (0.5 μm) as the effective diffusion dimension shows that a small amount of radiogenic ^{40}Ar has been lost as the $^{40}Ar/^{39}Ar$ age has been reset by ~0.5 Ma.